

Constraining the Location of Microlensing Objects towards the LMC through Parallax Measurement in EAGLE Observations

T. Sumi,¹ and Y. Kan-ya,²

¹*Princeton University Observatory, Princeton, NJ 08544-1001, USA; e-mail; sumi@astro.princeton.edu*

²*Division of Earth Rotation, National Astronomical Observatory of Japan, Tokyo 181-8588, Japan; e-mail:yukitoshi.kan-ya@nao.ac.jp*

Accepted Received in original form

ABSTRACT

We investigate the possibility of determining whether microlensing objects towards the Large Magellanic Cloud (LMC) are in a Galactic thick disc, or are in a Galactic halo, by using parallax measurements with an Earth-radius scale baseline. Our method makes use of EAGLE (Extremely Amplified Gravitational LEnsing) events which are microlensing events with an invisible faint source. We show that the rate of EAGLE events is as high as that of normal microlensing events, even if they are caused by dark stars in the Galactic thick disc. We explore the possibility of measuring the parallax effect in EAGLE events towards the LMC by using the *Hubble Space Telescope* (HST) or the *Very Large Telescope* (VLT). We find that EAGLE events enlarge the opportunity of parallax measurements by 4 \sim 10 times relative to that in normal microlensing events. We show that the parallax effect can be measured in \sim 75% (from the HST) and \sim 60% (from the VLT) of all EAGLE events if most lenses are stars in the Galactic thick or thin disc, while \sim 20% (from the HST) and \sim 10% (from the VLT) can be measured if most lenses are halo MACHOs. In combination with the finite source size effect observations, we can strongly constrain the location of lenses.

Key words: dark matter—Galaxy:halo—gravitational lensing—Magellanic Cloud

1 INTRODUCTION

Several groups have carried out gravitational microlensing observations towards the Large Magellanic Cloud (LMC) in order to search for MAssive Compact Halo Objects (MACHOs) in the Galactic halo. Until now, 13-17 candidates have been found towards the LMC and the microlensing optical depth τ from the events is $1.2^{+0.4}_{-0.3} \times 10^{-7}$ (Alcock et al. 2000b). The estimated typical lens mass depends on the adopted Galactic kinematic model ranging over 0.01 – 1 M_{\odot} (Alcock et al. 2000b; Honma & Kan-ya 1998).

We have learned that there are lens objects along the line of sight towards the LMC. However, the issues of where lens objects are and what they are, are still unclear. This is because a degeneracy occurs in ordinary microlensing events for which the amplification is described by (Paczynski 1986)

$$A(u) = \frac{u^2 + 2}{u\sqrt{u^2 + 4}} \sim \frac{1}{u} \text{ for } u \ll 1, \quad (1)$$

where u is the projected separation of the source and lens in units of the the Einstein radius R_E , which is given by

$$R_E(M, x) = \sqrt{\frac{4GM}{c^2} D_s x(1-x)}. \quad (2)$$

Here M is the lens mass, $x = D_d/D_s$ is the normalized lens distance and D_d and D_s are the observer-lens and the observer-source star distances. D_s is hereafter assumed to be 50 kpc. The time variation of the parameter $u = u(t)$ is

$$u(t) = \sqrt{\beta^2 + \left(\frac{t-t_0}{t_E}\right)^2}, \quad (3)$$

where β , t_0 , $t_E = R_E(M, x)/v_t$ and v_t are the minimum impact parameter in units of R_E , the time of maximum magnification, the event time-scale and the transverse velocity of the lens relative to the line of sight towards the source star, respectively. From a light curve, one can determine the value of β , t_0 and t_E , where M , x and v_t are degenerate in t_E . This three-fold degeneracy is the essential difficulty in determining the nature of the lens objects. There are only marginally possible candidates, viz. old white dwarfs (Alcock et al. 1997, 2000b; Hansen 1998), old brown dwarfs (Honma & Kan-ya 1998) and primordial black holes (Ioka, Tanaka & Nakamura 2000).

Possibilities for non-halo lensing objects have also been discussed, for example, dark objects in a dark heavy component of the LMC itself (Aubourg et al. 1999; Gyuk, Dalal & Griest 2000; Alcock et al. 2001). There is also the possi-

bility that the lenses are dark objects in the Galactic thick disc. While the microlensing optical depth τ by known populations of stars in the Galactic thin disc and thick disc is of order 10^{-9} (Alcock et al. 2000b), a maximal heavy thick disc, which may be surrounded by an extended dark halo composed of particles, is also a possible Galactic component as the reservoir of lenses (Gates, Gyuk & Turner 1995; Gates, et al. 1998). Such a thick disc can have $\tau \simeq 7 \times 10^{-8}$ (Gould 1994a; Gould, Miralda-Escude & Bahcall 1994), so the summed optical depth including the contribution from the Galactic thin disc ($\sim 2 \times 10^{-8}$) and the LMC itself ($\sim 1 \times 10^{-8}$, Sahu 1994) can be close to the observed value.

The three-fold degeneracy can be resolved in some kinds of exotic microlensing events, e.g., the binary event (Hardy & Warker 1995; Albrow et al. 1999; Alcock et al. 1999a; Honma 1999; Afonso et al. 2000; An & Gould 2001) and the finite source transit event (Gould 1992, 1994a; Nemiroff & Wickramasinghe 1994; Witt & Mao 1994; Peng 1997). Sumi & Honma (2000) pointed out that an extensive transit events search would make it possible to discriminate between the lenses in the Galactic halo and in the LMC.

The third example is an event with parallax effect, which is essentially detected through the difference of light curves due to the spatial shift of an observer or observers. In such events we could determine the “reduced transverse velocity” $\tilde{v} = v_t/(1-x)$ of the lens. Examples of the parallax effects are the following. The annual parallax effect due to the Earth’s motion around the Sun during an event leads an asymmetry in the light curve (e.g. Gould 1992; Gould, Miralda-Escude & Bahcall 1994; Miyamoto & Yoshii 1995; Alcock et al. 1995; Mao 1999; Bennett et al. 2001; Bond et al. 2001; Soszyński et al. 2001; Smith, Mao & Woźniak 2002; Mao et al. 2002). However, such events are rare. This parallax effect generally requires $t_E > \sim 100$ days, while $t_E \sim 40$ days for typical events. Another effect is parallax by the positional difference of two well-separated observation sites. In this case, we could measure the relative difference of the peak amplifications and the time at the peak amplifications between both. By observing an event from both a solar-orbit satellite and the Earth, we could utilize the parallax effect in almost every event, while it is difficult from two distant observatories on the Earth (Refsdal 1966; Gould 1994b, 1995b; Holz & Wald 1996). Furthermore, the parallax could be measured by the positional shift of an observer due to the diurnal motion of the Earth, which was first advanced by An et al. (2002), and due to the orbital motion of an Earth-orbit space telescope such as the *Hubble Space Telescope* (HST) (Honma 1999) in binary events. In ordinary microlensing events this effect is quite small, but it is more efficient around the peak of high magnification events.

For Galactic bulge events, Gould (1997) discussed the possibility of detecting the finite source size and parallax effects by using two distinct ground-based telescopes in order to break the degeneracy in EME’s (Extreme Microlensing Events, $A > 200$). With an approximate estimate for EME observations towards the LMC, he concluded that it is not feasible. However, with a more careful estimate, Nakamura & Nishi (1998) showed that it is feasible to detect EAGLE (Extremely Amplified Gravitational LEnsing) towards the LMC. EAGLE is similar to the so-called “Pixel lensing” events (Gould 1996) but more simply defined as the events in which the source star is dimmer than observational limiting

magnitude (ex. $V_{obs} = 21 \sim 22$), and not concerned whether the source star is resolved or not. Some EAGLEs would be EME’s. EAGLE events could be efficiently detected with the “image subtraction method” or “Difference Image Analysis (DIA)” (Alard & Lupton 1998; Alard 2000; Alcock et al. 1999b, 2000a; Woźniak 2000; Bond et al. 2001), which has been recently developed and can perform more accurate photometry than DoPHOT and Pixel lensing method. So, we refer the term EAGLE in this paper.

If lens objects are in the thin or thick disc (disc events), R_E projected onto the observer plane from the source star,

$$\tilde{R}_E(M, x) \equiv \frac{R_E(M, x)}{1-x} \propto \sqrt{\frac{x}{1-x}}, \quad (4)$$

is much smaller than that for halo events. In this case the light curve is more sensitive to the small displacement of the observer position. Therefore the fraction of parallax-measurable EAGLE events out of all EAGLE events for disc events will be much larger than that for halo events. This fraction is useful to discriminate statistically whether the lens objects are mainly in the thick disc or not.

Here, we estimate the rate of parallax-measurable EAGLE events towards the LMC. In §2 we summarize the basic equations of EAGLE events. In §3 EAGLE event rates are estimated. In §4 and 5 we describe the measurement of parallax effect from space and ground telescopes, respectively. In §6 we calculate the fraction of parallax-measurable events. Discussion and conclusion are given in §7.

2 BASIC FORMULAE FOR EAGLE EVENTS

An EAGLE event is a microlensing event in which a source star is fainter than the observational limiting magnitude. A highly amplified faint source would be detected as a new star. Nakamura & Nishi (1998) showed that the EAGLE event rate is fairly high towards the LMC. However an EAGLE search has not been involved in the microlensing surveys based on a DoPHOT-type PSF fitting photometry, which only measure already detected stars.

A new CCD photometry method called DIA, in which an exposure frame is directly compared with a reference frame, enables much more accurate photometry at any place where any star isn’t identified on the reference. This is more powerful for detecting EAGLE events than the DoPHOT. Many EAGLE events are expected to be found by DIA.

2.1 Detection threshold

A dim invisible source star with V -band apparent magnitude V must be amplified brighter than EAGLE detection threshold V_{th} , which is slightly brighter than the observational limit V_{obs} . So, the threshold amplitude is written as

$$A_T(V) \equiv 10^{0.4(V-V_{th})}. \quad (5)$$

A corresponding threshold impact parameter $u_T = u_T(A_T(V))$ which is the largest impact parameter to be detected as an EAGLE event depends on V and V_{th} . This can be approximately written as (Nakamura & Nishi 1998)

$$u_T(V) \simeq 10^{-0.4(V-V_{th})}. \quad (6)$$

3 GALACTIC MODEL AND EVENT RATE

Here we give adopted models of the Galaxy and source stars, and estimate the event rate. Since only the relative event rate is discussed, common constant factors C , f , and the normalization of the luminosity function are not essential.

When we consider microlensing by lens objects in the maximal disc ('disc events'), we adopt an exponential disc as the mass density distribution for the Galactic thin and thick disc. Since the line of sight to the LMC is almost tangential to the azimuthal direction in the Galaxy, the mass density at the region efficient to microlensing is not strongly dependent on the Galactocentric radius r but only on the height from the disc plane z , as long as the disc scale height is much smaller than $r \simeq 8.5$ kpc. So we assume the disc density distribution only depends on z as

$$\rho(z) = \frac{\Sigma}{2h} \exp\left(-\frac{z}{h}\right), \quad (7)$$

where Σ is the local disc column density and h is the scale height of the disc. For the thin and thick disc we set $h_{\text{thin}} = 350$ pc and $h_{\text{thick}} = 1400$ pc respectively. A certain acceptable value is $\Sigma_{\text{thin}} \simeq 50 M_{\odot} \text{pc}^{-2}$ (cf. Kuijken & Gilmore 1989). If we adopt this value, due to the maximal disc limit of $\sim 100 M_{\odot} \text{pc}^{-2}$ estimated from the rotation speed of the Galaxy (Binney & Tremaine 1987), $\Sigma_{\text{thick}} \simeq 50 M_{\odot} \text{pc}^{-2}$ (Gilmore & Reid 1983; Gould 1994a; Gould, Miralda-Escude & Bahcall 1994). However, the value of the local column density for each disc may be different (cf. Kuijken & Gilmore 1989; Bahcall, Flynn & Gould 1992; Creze et al. 1998; Holmberg & Flynn 2000). So we take Σ as a model parameter assuming that the combined mass of the thin and thick discs does not exceed the maximal disc limit. We change the fraction of each component within this limit, i.e., $\Sigma_{\text{thin}}(\Sigma_{\text{thick}}) = 30(70), 50(50)$ and $70(30) M_{\odot} \text{pc}^{-2}$.

For the disc events we assume the power-law mass function $\phi(M)$ of lens objects defined by equations (9) and (10) in Sumi & Honma (2000). The number density of lens objects with the mass between M and $M + dM$ is given by $n(M, x)dM = f\rho(z(x))\phi(M)dM/M$, where f is the mass fraction of the lens objects to the total mass and is assumed to be constant. We take the upper limit of mass $M_u = 50 M_{\odot}$ and treat the lower limit M_l and the power-law index α_d as model parameters as $M_l = 0.1$ or $0.01 M_{\odot}$ and $\alpha_d = 2.35$ or 5, i.e., we assume both the ordinary (Salpeter IMF) and an extreme model for a darker population of stars as a constituent of the maximal disc. Our main results do not depend on this index very much (see § 6). For the luminosity function of the source stars in the LMC, $\phi_L(V)$, we follow equations (15) and (16) in Sumi & Honma (2000) with the IMF index $\alpha_s = 2.35$, which is consistent with the luminosity function of the LMC observed by using the HST (Holtzman 1997).

For MACHOs ('halo events'), we adopt the spherical 'standard' halo model given by (Alcock et al. 2000b)

$$\rho_{\text{halo}}(r) = \rho_0 \frac{a^2 + r_0^2}{a^2 + r^2}, \quad (8)$$

where $\rho_0 = 0.0079 M_{\odot} \text{pc}^{-3}$ is the local mass density, r is the Galactocentric radius, $r_0 = 8.5$ kpc is the Galactocentric distance of the Sun, and $a = 5$ kpc is the core radius. We adopt delta-function mass functions with $M = 0.1$ and $0.5 M_{\odot}$ because the lens mass function is not well known.

For the observational parameters we assume $V_{\text{obs}} = 21$,

which is a typical value for current microlensing programs with a 1-m class telescope. The events with the source star having $V < 21$ are normal microlensing events, while ones with $V > 21$ are EAGLE events. We consider two different values for the threshold magnitude; $V_{\text{th}} = 19$ and 20.

The event rates of normal microlensing events (Γ_N) and EAGLEs (Γ_E), which are proportional to R_E and $u_T R_E$ respectively, are given by

$$\Gamma_N = C \int_0^1 D_s dx \int_{V_l}^{V_{\text{obs}}} dV \int_{M_l}^{M_u} dM R_E v_t \phi_L(V) n(M, x), \quad (9)$$

$$\Gamma_E = C \int_0^1 D_s dx \int_{V_{\text{obs}}}^{V_u} dV \int_{M_l}^{M_u} dM u_T R_E v_t \phi_L(V) n(M, x), \quad (10)$$

where $V_u = 30$ and $V_l = 16$ are the upper and lower limit of the luminosity function. Note that the integration is performed $V < V_{\text{obs}}$ for Γ_N and $V > V_{\text{obs}}$ for Γ_E .

We calculate the relative EAGLE event rate Γ_E/Γ_N for disc events, with the finite source size effect included. The results for $V_{\text{th}} = 19$ and 20 are $\Gamma_E/\Gamma_N = 0.73$ and 1.83, respectively, only weakly dependent on parameters of the disc structure (Σ, h) and the mass function (α_d, M_l). This ratio depends on the luminosity function of source stars. As a result, only in the most extreme case that $V_{\text{th}} = 19$, $\alpha_d = 5.0$ and $M_l = 0.01 M_{\odot}$, this ratio is slightly decreased due to finite source size effects. In the case that $V_{\text{th}} = 20$ and $\alpha_d = 2.35$, we found that this effect is not negligible only when $M_l < 10^{-4}$. For halo events, the events affected by finite source size effects are only several percent out of all EAGLE events (Sumi & Honma 2000). So hereafter we neglect the finite source size effect.

For events in which the source star is $V > 25$, the period in which the source is visible ($V < 21$) is less than 2 days. Then the detection efficiency for such events should be very low. So we estimated Γ_E/Γ_N in the case that the source star is $V < 25$, and found $\Gamma_E/\Gamma_N = 0.59$ and 1.47 with $V_{\text{th}} = 19$ and 20, respectively. We checked this ratio in the conservative case of a gentler slope $\alpha_s = 2.0$ with $V_{\text{th}} = 20$ and $V < 25$, and found it to be 1.15. This is still sufficiently high.

In this paper, we assume that microlensing events (normal and EAGLE) would be detected by a 1-m class alert telescope and the real-time analyses with DIA, and then follow-up observations would be performed by an Earth-orbit space telescope or a large ground-based telescope.

4 PARALLAX FROM SPACE TELESCOPE

Here we describe the parallax effect observed with an Earth-orbit space telescope such as the HST. In the following analysis, we use the coordinate system which is used in Honma (1999), i.e., the origin is set to be the centre of the Earth, and z -axis is set to be in the direction of the source star. The x -axis is set to be perpendicular to both of the z -axis and the orbital axis of the space telescope. The inclination i of the telescope orbit is defined as an angle between the z -axis and the orbital axis. We also assume that the space telescope is in a circular orbit with radius r_{st} and angular velocity ω . The position of the telescope projected onto the observer plane (x - y plane) is written as

$$\mathbf{T} = [r_{\text{st}} \cos(\omega t + \delta), r_{\text{st}} \sin(\omega t + \delta) \cos i]. \quad (11)$$

Here the angle δ describes the position of the space telescope at $t = t_0$. Observed from the centre of the Earth, the position of the lens object on the lens plane is given by

$$\mathbf{L_E} = [v_t(t - t_0) \cos \theta - b \sin \theta, v_t(t - t_0) \sin \theta + b \cos \theta], \quad (12)$$

where θ is the angle between the x -axis and the direction of the transverse velocity of the lens v_t and b is the minimum physical distance between the lens and the source-Earth line of sight. The position of the lens relative to the space telescope on the lens plane is given by

$$\mathbf{L_T} = \mathbf{L_E} - (1 - x)\mathbf{T}. \quad (13)$$

Then from the space telescope $u(t)$ is written as

$$u'(t)^2 = \left\{ \frac{1}{t_E}(t - t_0) \cos \theta - \beta \sin \theta - \epsilon \cos(\omega t + \delta) \right\}^2 + \left\{ \frac{1}{t_E}(t - t_0) \sin \theta + \beta \cos \theta - \epsilon \sin(\omega t + \delta) \cos i \right\}^2, \quad (14)$$

where $\epsilon = r_{st}/\tilde{R}_E$. Equation (14) shows that the parallax effect due to the telescope motion causes a wavy trajectory of the lens object relative to that from the centre of the Earth. For orbital parameters for the space telescope, we assumed $r_{st} = 7000$ km, $i = 30^\circ$ and $P_{orb} = 2\pi/\omega = 97$ min, which are similar to those of the HST.

We show sample light curves without ($A(u)$, thin line) and with ($A(u')$, thick line) the parallax in Fig. 1a, as well as the difference of the two $\delta A = A(u') - A(u)$ in Fig. 1b in the case with $t_E = 5$ days, $v_t = 30$ km s $^{-1}$, $x = 0.01$, $\beta = 0.05$, $\theta = 90^\circ$ and $\delta = 0^\circ$. Hereafter in the case using the HST, we take $\delta = 0^\circ$ since δ is a random parameter related with just a phase of orbit. We ensured that this does not affect our main results. In the light curve from the space telescope, the small wavy perturbation from that observed from the centre of the Earth can be seen. In the δA light curve in Fig. 1b, we can clearly see that the fluctuation due to the parallax is enhanced around the peak.

From the observation, we can derive the ϵ and θ in addition to other parameters t_E , β , t_0 and f_0 . From ϵ and t_E we can derive the “reduced velocity” \tilde{v} as follows

$$\tilde{v} = \frac{r_{st}}{\epsilon t_E}. \quad (15)$$

The reduced transverse velocity represents the projected relative transverse velocity between the source star and the lensing object and will be of great use in investigating the lens location because this value for each component (halo, thick disc, and thin disc) is different (about 240 km s $^{-1}$, 50 km s $^{-1}$ and 30 km s $^{-1}$, respectively) and hence for disc events \tilde{v} is ~ 8 times smaller than that for halo events.

The rate of parallax-measurable microlensing events depends on the uncertainty of \tilde{v} which is given by

$$\begin{aligned} \sigma_{\tilde{v}} &= \left\{ \left(\sigma_\epsilon \frac{\partial \tilde{v}}{\partial \epsilon} \right)^2 + \left(\sigma_{t_E} \frac{\partial \tilde{v}}{\partial t_E} \right)^2 \right\}^{\frac{1}{2}} \\ &= \tilde{v} \left\{ \left(\frac{\sigma_\epsilon}{\epsilon} \right)^2 + \left(\frac{\sigma_{t_E}}{t_E} \right)^2 \right\}^{\frac{1}{2}}, \end{aligned} \quad (16)$$

where σ_ϵ and σ_{t_E} are the errors in the ϵ and t_E . We assume that the required threshold accuracy to measure \tilde{v} due to the parallax effect is 50%, i.e., $\sigma_{\tilde{v}}/\tilde{v} < 1/2$, in this paper.

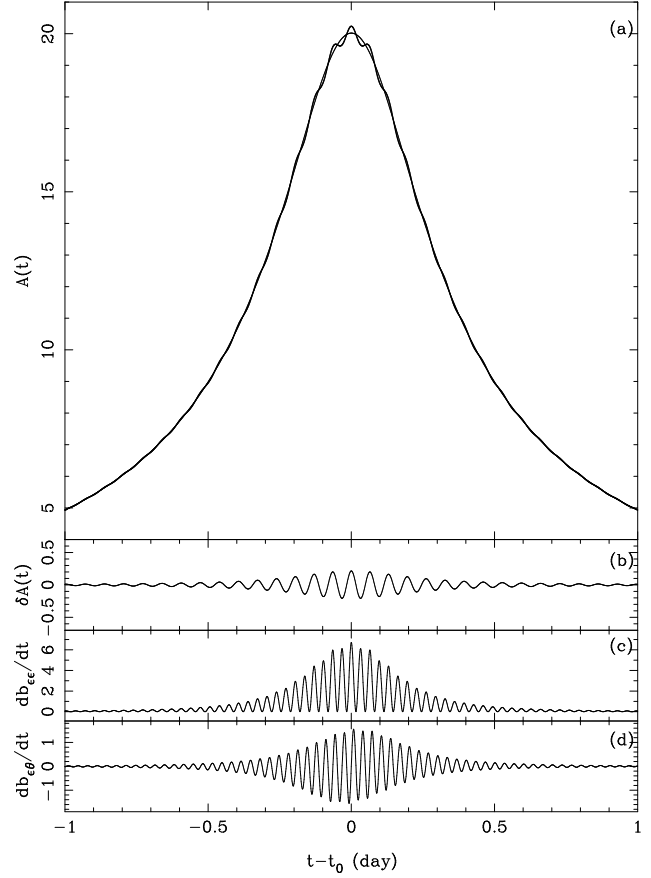


Figure 1. (a) Light curves observed from the centre of the Earth (thin line) and from the HST (thick line), (b) δA light curve, (c) and (d) show integrands of the $b_{\epsilon\epsilon}$ and $b_{\theta\theta}$, i.e. $\partial b_{\epsilon\epsilon}/\partial t$ in 10^{10} e $^{-}$ day $^{-1}$ and $\partial b_{\theta\theta}/\partial t$ in 10^7 e $^{-}$ day $^{-1}$ respectively, in the case of $t_E = 5$ days, $v_t = 30$ km s $^{-1}$, $x = 0.01$, $\beta = 0.05$, $\theta = 90^\circ$ and $\delta = 0^\circ$. The amplitude of the modulation depends on ϵ .

The general discussion to estimate the error or the variance of a set of parameters a_i in fitting a distribution $F(t, a_i)$ is presented by, e.g., Gould (1995a, 1998) using the minimum variance bound given from a well-known theorem in statistics. The covariance matrix c_{ij} with respect to a_i for a series of measurements $F(t_k)$ at time t_k with error σ_k is given by

$$c_{ij} = b_{ij}^{-1}, \quad b_{ij} = \sum_k \sigma_{F(t_k)}^{-2} \frac{\partial F(t_k)}{\partial a_i} \frac{\partial F(t_k)}{\partial a_j}. \quad (17)$$

The variance of a_i is just the diagonal elements c_{ii} .

We take $F(t)$ as the number of the detected photo-electrons at time t from the source star. During a short time interval T , we get $F(t) = (f_0(V)A(t; \beta, t_E, t_0) + f_b)T$, where f_0 denotes the average photo-electron flux from the unamplified source star and f_b denotes the background flux in the PSF aperture from the sky and the unlensed blending stars. $A(t; \beta, t_E, t_0)$ is the amplification produced by microlensing given by equations (1) and (3). By using the DIA, the signal is expressed as $\Delta F(t) = f_0(A - 1)$ and $\sigma_F(t) = \sqrt{F(t)}$. Taking the limit $T \rightarrow 0$, b_{ij} in equation (17) is given by

$$b_{ij} \simeq \int_{t_{\text{begin}}}^{t_{\text{end}}} \frac{1}{f_0(V)A + f_b} \left[\frac{\partial f_0(A - 1)}{\partial a_i} \right] \left[\frac{\partial f_0(A - 1)}{\partial a_j} \right] dt. \quad (18)$$

A parallax effect tends to be measured accurately in the case that f_0 is large, and/or β , v_t , x and/or M are small.

We show the integrands of $b_{\epsilon\epsilon}$ and $b_{\epsilon\theta}$ in Fig. 1c and 1d, respectively, in the case of the source magnitude of $V = 21$ and with the same parameters as in Fig. 1a. Here we assumed $f_0(V = 20) = 350 \text{ e}^- \text{ s}^{-1}$ and $f_b = 10 \text{ e}^- \text{ s}^{-1}$, which is similar to those of the HST with the *Advanced Camera for Surveys* (ACS) (Pavlovsky 2001). f_b in the aperture of the PSF is estimated by taking account of the following sources; (1) Zodiacal light $V_{\text{ZL}} = 23.3 \text{ mag arcsec}^{-2}$, which is the smallest because the Ecliptic latitude of the LMC is $\sim 90^\circ$. (2) Earth shine from the limb of the sunlit Earth $V_{\text{ES}} = 21.4 \text{ mag arcsec}^{-2}$, which is the mean when the angle θ_{limb} between the target and the bright Earth limb is larger than 12° . (3) Light from Blending stars $V_{\text{LMC}} = 22.01 \text{ mag arcsec}^{-2}$, which is the mean V -band surface brightness of the inner 10 deg^2 of the LMC (de Vaucouleurs 1957). We reduced $f_0(V)$ and f_b by a factor of $3/4$ because the LMC could not be observed when the HST is in shadow of the Earth and we limit $\theta_{\text{limb}} > 12^\circ$. (Note: the phase when the observation would be interrupted is not always the same, because the actual orbit of the HST is not circle but the latitude of the HST is changing between -30° and 30° .) We multiplied $f_0(V)$ and f_b by 0.9 taking account of the dead time of camera assuming ~ 5 minutes exposures.

In Fig. 1c and 1d, we can see that most of the information of ϵ is in very short period ($\sim t_E \beta$) around the peak, and the correlation between ϵ and θ , i.e., $b_{\epsilon\theta}$ is negligible in a day-period observation. Furthermore, we ensured that ϵ is completely independent of other parameters.

We assume that the follow-up observation for EAGLE events would be carried out by the HST for one day from t_0 . The extensive follow-up observations from ground-based small telescopes around the world make it possible to know t_0 . We evaluate the uncertainty of the parameters σ_{a_i} ($a_i = \epsilon, \theta, t_E$). In Fig. 2, we show σ_{a_i}/a_i as a function of β for the case of the typical event time-scale of $t_E = 40$ days with same parameters used above except for $\theta = 45^\circ$. The σ_ϵ is the minimum at $\theta = 90^\circ$ and the maximum at $\theta = 0^\circ$. Hereafter, we fixed $\theta = 45^\circ$ since θ is a random parameter. We ensured that the difference of the main results in §6.2 between the case using fixed $\theta = 45^\circ$ and the case taking θ at random, is negligible.

Meanwhile t_E is highly correlated with other parameters, i.e., β , t_0 and f_0 . If the event is observed symmetrically in time around t_0 , t_E is completely independent of t_0 because t_0 is an odd parameter in time. However, in the case that the event would be observed for a day from t_0 , t_E is no longer independent of t_0 . In Fig. 2 we show (i) σ_{t_E}/t_E (dotted line) and σ_{t_E}/t_E under the condition that (ii) f_0 (3dotted-dashed line) or (iii) both f_0 and t_0 (dot-dashed line) are externally constrained. This (i) σ_{t_E} in which there is a f_0 would be much improved over using two different telescopes to measure the parallax in which there are two f_0 . Though, comparing (i) and (ii), the former one deteriorates relative to the latter one because of degeneracies among the parameters t_E , β and f_0 , which is severe in the case that the event is observed only around the peak (Gould 1997; Han 1997). This can be improved by constraining f_0 by follow-up observation with the HST after the event (Han 1997). Hereafter we assume that f_0 would be constrained by the follow-up observation. As shown in Fig. 2, case (ii) is larger than (iii),

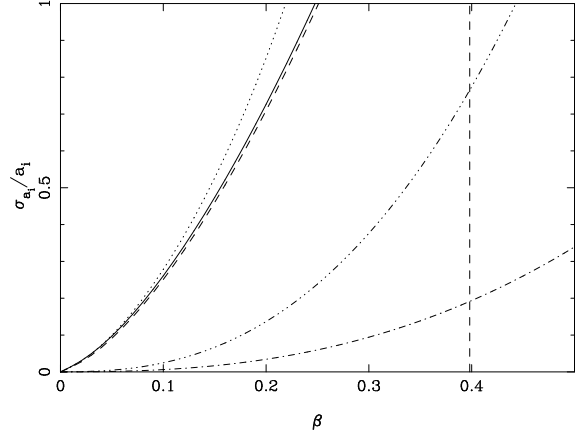


Figure 2. Uncertainty σ_{a_i}/a_i as a function of the impact parameter β for ϵ (solid line), θ (dashed line), (i) t_E (dotted line) and t_E under the condition that (ii) f_0 (3dotted-dashed line) or (iii) both f_0 and t_0 (dot-dashed line) are externally constrained, in the case of $t_E = 40$ days, $x = 0.01$, $v_t = 30 \text{ km s}^{-1}$, $\theta = 45^\circ$ and the source magnitude $V = 21$. The vertical dashed line indicates the EAGLE detection threshold impact parameter u_T .

but still quite small relative to σ_ϵ/ϵ . Especially in the region of $\sigma_\epsilon/\epsilon < 1/2$, where we are concerned, σ_{t_E}/t_E is at least 10 times smaller than σ_ϵ/ϵ . In the case for brighter source event ($V < 21$), the contribution of σ_{t_E}/t_E becomes slightly larger at $\sigma_\epsilon/\epsilon \sim 1/2$, but in this case t_0 could be constrained well from the overall light curve taken by ground-based telescopes. Then hereafter we neglect σ_{t_E}/t_E in equation (16), i.e., we can rewrite equation (16) to $\sigma_{\tilde{v}}/\tilde{v} \simeq \sigma_\epsilon/\epsilon$.

From the curve of σ_ϵ/ϵ , we can obtain the critical impact parameter β_{crit} to detect an parallax effect with 50% accuracy, which corresponds to $\sigma_\epsilon/\epsilon = 1/2$.

5 PARALLAX FROM GROUND TELESCOPE

Here we consider parallax measurements from an 8-m class telescope at a latitude of -30° on the Earth such as the *Very Large Telescope* (VLT). In this case the light curve would be expressed with the same equation as that from the HST (see equation (14)) except that the radius of the orbit is $R_{\text{orb}} = R_\oplus \cos 30^\circ = 5500 \text{ km}$, the period is $P_{\text{orb}} = 2\pi/\omega = 1$ day and we can observe events only during night-time. Here R_\oplus is the Earth radius.

In Fig. 3, we show sample light curves of $\delta A = A(u') - A(u)$ (a and d) and integrands of $b_{\epsilon\epsilon}$ (b and e) and $b_{\epsilon\beta}$ (c and f) in the case of $t_E = 40$ days, $v_t = 30 \text{ km s}^{-1}$, $x = 0.01$ and $\beta = 0.05$. Here we assumed that observations are performed for 7 hours a day. Fig. 1a-c and 1d-f represent the case that the dark-side of the Earth is near to the lens relative to the centre of the Earth, i.e. $\theta_N - \theta = 90^\circ$, and the case that $\theta_N = \theta$ respectively, where θ_N is the angle between the centre of the observation night relative to the centre of the Earth and the x-axis. In this case, we can observe only some parts of the wavy light curve, and then ϵ is highly correlated with other parameters, i.e., θ , t_E , β , t_0 and f_0 . In the case of Fig. 3a-c, $b_{\epsilon\beta}$ becomes large as well as $b_{\epsilon\epsilon}$, then σ_ϵ becomes significantly larger than the case of Fig. 3d-f in which $b_{\epsilon\beta}$ becomes quite small, as well as the other cross terms b_{ij} .

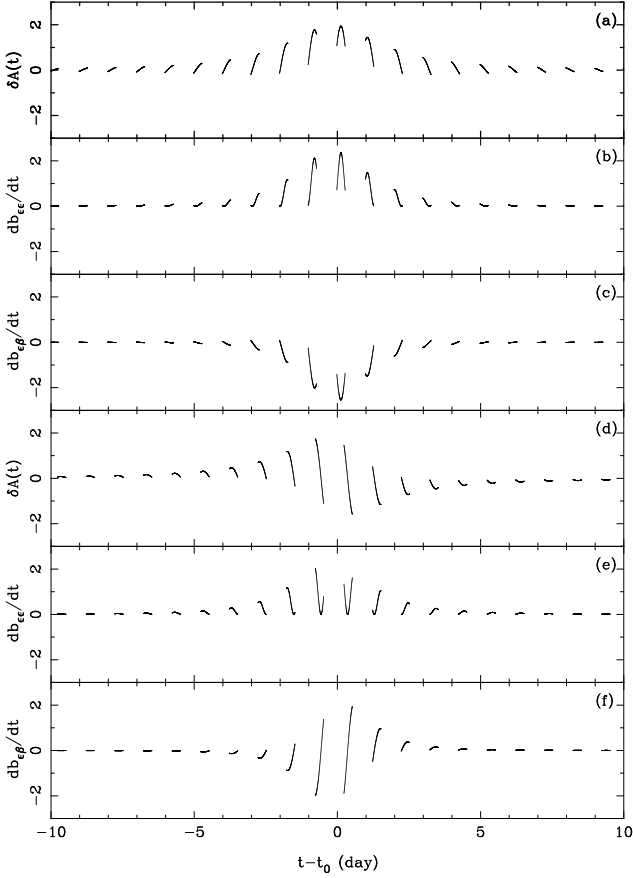


Figure 3. Light curves of δA (a and d) in 10^{-2} and integrands of b_{ϵ} (b and e) and b_{β} (c and f) in 10^{-11} in the case of $t_E = 40$ days, $v_t = 30 \text{ km s}^{-1}$, $x = 0.01$, $\beta = 0.05$ and the source magnitude $V = 21$. Panels (a)-(c) and (d)-(f) represent the cases of $\theta_N - \theta = 90^\circ$, and the case of $\theta_N = \theta$ respectively.

We estimate σ_ϵ by the same procedure in § 4, i.e. evaluating the covariant matrix. In this case, we assume the photo-electron flux is $f_0(V = 20) \simeq 2000 \text{ e}^- \text{ s}^{-1}$ using an 8-m class telescope and thin CCD cameras with a filter near the V band with a relatively narrow bandwidth ($\sim 100 \text{ nm}$). The very broad-band filter is not advisable because that might not be able to eliminate the effect of differential refraction or differential extinction of the atmosphere (Gould 1998). We reduce $f_0(V)$ and f_b by a factor of 2 to take account of weather conditions and CCD camera dead time. We adopt the background flux $f_b = 1200 \text{ e}^- \text{ s}^{-1}$ corresponding to $V = 20.6$ mag, which is estimated as follows: the mean V-band surface brightness of the inner 10 deg^2 of the LMC is $V = 22.01 \text{ mag arcsec}^{-2}$, and the sky value is $V = 21.6 \text{ mag arcsec}^{-2}$ (de Vaucouleurs 1957). We assume the aperture of the PSF is $0.49\pi \text{ arcsec}^2$ ($\sim 0.7''$ seeing) which is similar to the typical seeing of the VLT. The total brightness in the aperture is 20.6 mag. We adopt this value for f_b . Here we assumed that the follow-up observation would be taken for three nights (7 hours a night) around the peak.

The LMC is visible enough (~ 7 hours) only during the southern summer (between equinoxes) from the site at a latitude of -30° , which corresponds to that θ_N is distributed at random between $0^\circ \sim 180^\circ$. σ_ϵ is maximum at $\theta_N = 0^\circ$ and

180° and minimum at $\theta_N = 90^\circ$ because of the inclination of the orbit axis $i = 30^\circ$. Hereafter we use the mean value of $\theta_N = 45^\circ$. We ensure that the difference of the main results in the following analyses between the case using the fixed $\theta_N = 45^\circ$ and that using a random θ_N is negligible. Anyway, this effect is much smaller than the dependence on $\theta - \theta_N$.

In Fig. 4, we show σ_ϵ/ϵ under the condition that f_0 is externally constrained (thick line), σ_ϵ/ϵ under the condition that all other parameters are externally constrained (thin line), which is shown to compare with the case using the HST, and σ_{tE}/t_E under the condition that f_0 is externally constrained (dashed line) as a function of β in the case of $t_E = 40$ days, $x = 0.01$, $v_t = 30 \text{ km s}^{-1}$, $\theta_N = 45^\circ$, $\delta = 45^\circ$ and the source magnitude of $V = 21$. Upper and lower panels represent the case of $\theta = -45^\circ$ (i.e. $\theta_N - \theta = 90^\circ$, which correspond to Fig. 1a-c) and the case of $\theta = 45^\circ$ (i.e. $\theta_N = \theta$, which correspond to Fig. 1d-f), respectively. In this figure, $\sigma_{\bar{v}}/\bar{v}$ heavily depends on $\theta_N - \theta$, it especially deteriorates in the case of $\theta_N - \theta = 90^\circ$ relative to the thin line. In this case σ_{tE}/t_E is also negligible.

$\delta = 45^\circ$ is the most optimal case, i.e. one observes the peak at θ_N in the second observation night. In actual δ depends on random parameters t_0 and θ_N , and how early one can start the follow-up. Fig. 5 show σ_ϵ/ϵ as a function of δ in the case using same parameters in Fig. 4 and $\beta = 0.04$, for the source magnitude of $V = 20, 21, 22, 23$ and 24 (from bottom to top). Here we take the mean value of σ_ϵ/ϵ over $-45^\circ < \theta < 135^\circ$ because the θ at which σ_ϵ/ϵ is the maximum or minimum, is related with δ . In Fig. 5 we can see σ_ϵ/ϵ does not depend on δ very much, as long as observations are spread roughly around t_0 , i.e. it does not need to cover the peak exactly. When the follow-up observation is delayed more than 1 day ($\delta < \sim -300$), it becomes worse especially for dimmer source events. This is worse for shorter time-scale events with much smaller β because most of the information of the parameters is contained in a very short period ($\sim t_E\beta$) around the peak. Furthermore in extreme cases ($t_E \ll 10$ days, $\beta \ll 0.01$), generally σ_ϵ/ϵ is small, however, it depends on whether the peak is covered exactly or not. This effect is large in dimmer source events ($V > 25$).

From the curve of σ_ϵ/ϵ we can also obtain β_{crit} . We take the mean of β_{crit} over $-45^\circ < \theta < 135^\circ$. Uncertainty σ_ϵ also depends on the direction of v_t . Note that this is negligible in the case using the HST. We take the mean of β_{crit} on the cases of $-v_t$ and $+v_t$ (i.e. same and opposite direction relative to the Earth rotation, respectively) in § 6.2.

6 FRACTION OF PARALLAX-MEASURABLE EVENTS

Here we calculate the fraction of parallax-measurable events out of all events in the case of $V_{\text{th}} = 20$ and $V_{\text{obs}} = 21$. We adopt the same Galaxy density model and the source luminosity function as § 3. To make the estimation realistic, we applied a photometric error 17% larger than the photon noise, which is estimated for the DIA (Woźniak 2000). Furthermore, we specify the typical (transverse) velocity of the lens objects to estimate parallax-measurable event rate.

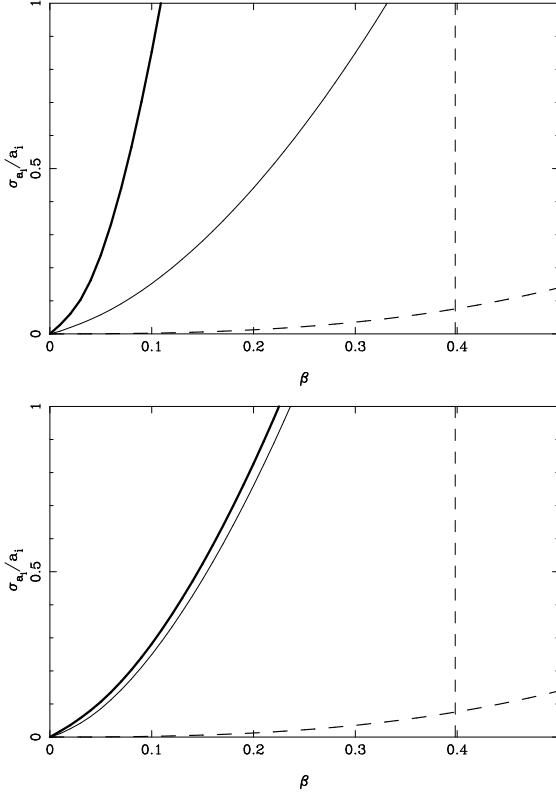


Figure 4. Uncertainty σ_ϵ/ϵ under the condition that f_0 (solid line) and all other parameters (dotted line) are externally constrained, and σ_{t_E}/t_E under the condition that f_0 is externally constrained (dot-dashed line) as a function of β in the case of $t_E = 40$ days, $x = 0.01$, $v_t = 30 \text{ km s}^{-1}$, $\theta_N = 45^\circ$, $\delta = 45^\circ$ and the source magnitude $V = 21$. Upper and lower panels represent the case of $\theta = 45^\circ$ (i.e. $\theta_N = \theta$, which correspond to Fig. 1a-c) and the case of $\theta = 135^\circ$ (i.e. $\theta_N - \theta = 90^\circ$, which correspond to Fig. 1d-f) respectively. The vertical dashed line indicates u_T .

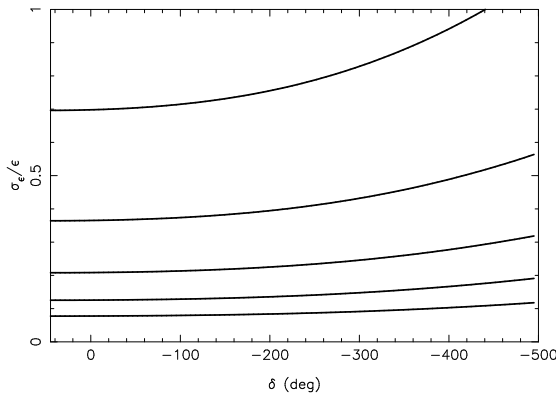


Figure 5. Uncertainty σ_ϵ/ϵ as a function of δ in the case of using the same parameters as Fig. 4 and $\beta = 0.04$, for the source magnitude of $V = 20, 21, 22, 23$ and 24 from bottom to top. Here smaller δ means that observations are delayed relative to the optimal case that the peak is observed at the centre of the second night ($\delta = 45^\circ$).

6.1 Model kinematics

For disc events the typical transverse velocity of a lens object v_t is estimated as follows. First we assume that the thin and thick discs have the same rotation velocity and the relative velocity between the mean flow of the lens objects and the local standard of rest (LSR) is zero. In fact the effect of the drift velocity of the thick disc relative to the thin disc due to the large velocity dispersion of the thick disc is negligible compared to other effects. v_t is the composition of the tangential component of the mean velocity of the Earth relative to the LSR v_\oplus and the velocity dispersion of the disc σ , which is assumed to be isotropic for both discs, as

$$v_t^2(z) = 2\sigma^2(z) + v_\oplus^2. \quad (19)$$

We take $v_\oplus = 30 \text{ km s}^{-1}$, which includes the orbital velocity of Earth around the Sun of 30 km s^{-1} and a velocity of the Sun relative to LSR of 20 km s^{-1} (Miyamoto & Zhu 1998). $\sigma^2(z)$ and v_t^2 are assumed to be a function of z only (see the discussion on equation (7)). The density profile of the disc is same as in §3, i.e., the exponential disc density distributions in equation (7) for thin ($h_{\text{thin}} = 350 \text{ pc}$) and thick ($h_{\text{thick}} = 1400 \text{ pc}$) discs with variable values of the local disc column density as $\Sigma_{\text{thin}}(\Sigma_{\text{thick}}) = 30(70), 50(50), 70(30) M_\odot \text{ pc}^{-2}$. Solving the Poisson equation for the density profile composed of the thin and the thick discs $\sigma^2(z)$ is obtained from the z -component of the Jeans equation (e.g. Binney & Tremaine 1987) as

$$\sigma^2(z) = \frac{\pi G}{2} \frac{\left[\Sigma_{\text{thin}} \exp\left(-\frac{z}{h_{\text{thin}}}\right) + \Sigma_{\text{thick}} \exp\left(-\frac{z}{h_{\text{thick}}}\right) \right]^2}{\rho_{\text{thin}}(z) + \rho_{\text{thick}}(z)}. \quad (20)$$

For halo events we adopt the same model as in §3 and we assume $v_t = 190 \text{ km s}^{-1}$ or 220 km s^{-1} . $v_t = 190 \text{ km s}^{-1}$ is more plausible because of the slight contribution from the disc gravity to the rotation curve, which is assumed to be flat with $v_{\text{rot}} = 220 \text{ km s}^{-1}$.

6.2 Results

We estimate the relative parallax-measurable event rate. The parallax-measurable event rate is written as

$$\Gamma_P = C \int_0^1 D_S dx \int_{V_l}^{V_u} dV \int_{M_l}^{M_u} dM \beta_{\text{crit}}(V, M, x, v_t(z(x))) R_E v_t \phi_L(V) n(M, x), \quad (21)$$

where C is the constant common to the expression of Γ_N (equation (9)) and Γ_E (equation (10)). And $V_u = V_{\text{obs}}$ for the normal events and $V_l = V_{\text{obs}}$ for EAGLEs. β_{crit} is estimated by same procedure presented in §4 and 5 for each parameter.

In Fig. 6 we show the relative event rate distributions of parallax-measurable events $d\Gamma_P/dV$ from the HST (upper panel) and from the VLT in the case of $\delta = 45^\circ$ (lower panel), normalized by Γ_N (for $V < V_{\text{obs}}$) or Γ_E (for $V > V_{\text{obs}}$) for thin disc, thick disc and halo events, as a function of source magnitude V and for various combinations of M_l and α_d . We note that the absolute value of the vertical axis is not important because these distributions are relative ones. These distributions are to be compared with the relative event rate distribution for all events (the bold dotted line). The left side relative to the vertical dashed line corresponds to normal microlensing events and the right side

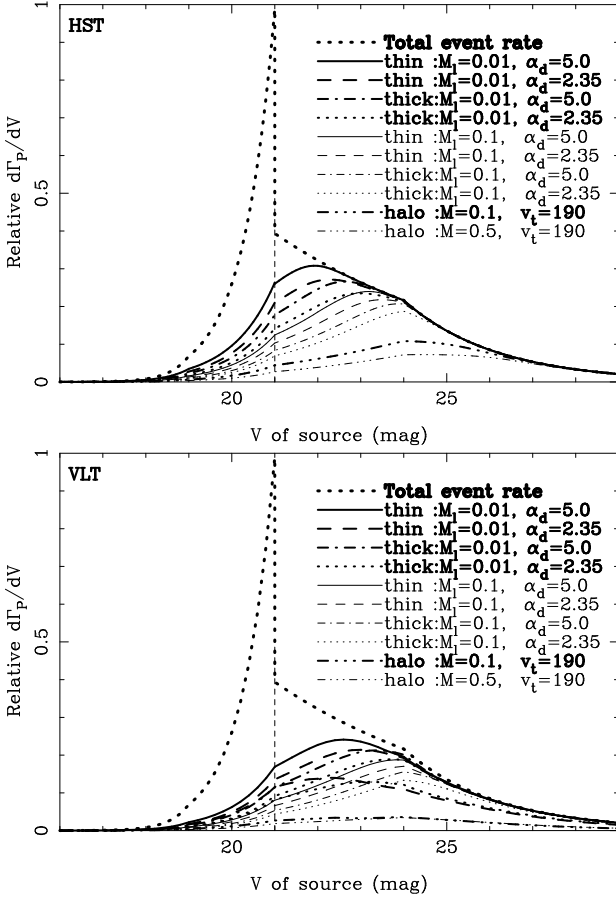


Figure 6. Relative differential event rate distribution of parallax-measurable events $d\Gamma_P/dV$ from the HST (upper panel) and from the VLT in the case of $\delta = 45^\circ$ (lower panel), normalized by Γ_N (for $V < V_{\text{obs}}$) or Γ_E (for $V > V_{\text{obs}}$), as a function of source magnitude V and for various combinations of M_l and α_d . By the VLT, for a comparison, we also show that distributions in the case of $\delta = -367.5^\circ$ (i.e. the case that the observation start at t_0) for two cases of the thin and thick discs with $M_l = 0.01$ and $\alpha_d = 2.35$ as same line styles (lower one). We also show the relative $d\Gamma_N/dV$ and $d\Gamma_E/dV$ by the bold dotted line.

is for EAGLE events. For disc events the greater α_d or the smaller M_l , the higher $d\Gamma_P/dV$ is. From Fig. 6 we can see that the event rate of parallax-measurable EAGLE events ($V > 21$) is much higher than that of normal microlensing events ($V < 21$). We can also see that for halo events the fraction of parallax-measurable events is still quite low even in EAGLE events. From the VLT (lower panel), we also show that distributions in the case of $\delta = -367.5^\circ$ (i.e. the case that the observation starts at t_0) for two cases of the thin and thick discs with $M_l = 0.01$ and $\alpha_d = 2.35$ as same line styles (lower one). From this figure, we can see that follow up observations by the VLT should be started ~ 1 day before t_0 to detect the parallax efficiently. Hereafter, we assume $\delta = 45^\circ$ for the case using the VLT.

We evaluate the ratio of the parallax-measurable EAGLE event rate to the parallax-measurable normal event rate $\Gamma_P(V > V_{\text{obs}})/\Gamma_P(V < V_{\text{obs}})$ in Table 1 for disc events with $\Sigma_{\text{thin,thick}} = 50 M_\odot \text{pc}^{-2}$ and in Table 2 for halo events with the lens mass of $M = 0.1$ and $0.5 M_\odot$ in the case of $V < 25$ mag. From Table 1 and 2, it is clear that EAGLE

Table 1. Ratio of the parallax-measurable EAGLE event rate to the parallax-measurable normal event rate for disc events.

α_d	the thin disc $M_1 = 0.1 M_\odot \quad M_1 = 0.01 M_\odot$		the thick disc $M_1 = 0.1 M_\odot \quad M_1 = 0.01 M_\odot$	
HST				
2.35	7.30	4.70	8.56	6.03
5.0	6.71	4.05	8.07	5.36
VLT				
2.35	8.44	5.78	9.50	7.24
5.0	7.90	5.11	9.22	6.59

Table 2. Ratio of parallax-measurable event in EAGLE events to that in normal events for halo events.

$v_t = 190 \text{ km s}^{-1}$		$v_t = 220 \text{ km s}^{-1}$	
$M = 0.1 M_\odot$	$M = 0.5 M_\odot$	$M = 0.1 M_\odot$	$M = 0.5 M_\odot$
HST			
7.65	8.29	7.42	8.01
VLT			
4.58	6.17	4.20	5.76

events enlarge the opportunity of parallax measurements. The number of parallax-measurable EAGLE events is $5 \sim 9$ (from the HST) and $6 \sim 10$ (from the VLT) times larger than that of normal events for disc events. For halo events these are ~ 8 (from the HST) and $4 \sim 6$ (from the VLT) times larger than that of normal events. We hereafter refer Γ_P as the parallax-measurable EAGLE event rate because most of the parallax-measurable events are EAGLE events.

In Table 3 we show the fractions of parallax-measurable EAGLE events out of all EAGLE events Γ_P/Γ_E and corresponding mean event time-scales $\langle t_E \rangle$ for disc events in the case of $V < 25$ mag. For $\Sigma_{\text{thick}}(\Sigma_{\text{thin}}) = 30(70)$, $50(50)$ and $70(30) M_\odot \text{pc}^{-2}$, the optical depths are $3.84(2.43)$, $6.41(1.74)$ and $8.97(1.04)$ in 10^{-8} , respectively, if $f = 1$, although the common factor f is not essential so long as a relative event rate is discussed, as noted in § 3. From Table 3, we see that $\langle t_E \rangle$ is strongly affected by M_l . $M_l = 0.01 M_\odot$ seems to be consistent with the observed value $t_E \sim 40$ days (Alcock et al. 2000b) for the thick disc with $\alpha_d = 2.35$. Γ_P/Γ_E only depends weakly on $\Sigma_{\text{thin|thick}}$ and α_d ¹. We can see that the parallax effect can be measured in $\sim 75\%$ (from the HST) and $\sim 60\%$ (from the VLT) of EAGLE events if the lenses are stars in the thick disc.

The fractions for the thin disc are $\sim 10\%$ larger than that for the thick disc, though the contribution of these components is small because the optical depth is about 25% relative to that of the thick disc (Gould 1994a; Gould, Miralda-Escudé & Bahcall 1994). M_l might be between 0.1 and 0.01

¹ In our disc model, v_t is larger for the larger Σ_{thick} case, and so Γ_P/Γ_E tends to be smaller. However for the thick disc from the HST it is inverse, because $\Gamma_P \propto v_t$, which is large for small x and this effect is slightly larger than the former effect in this case. Anyway, these effects are quite small relative to the others we are concerned.

Table 4. Fraction of parallax-measurable events in all EAGLE events and mean time-scales for halo events with mass functions, $\delta(M)$: the delta-function with mass M , $G(M)$: the Gaussian and $G(\log M)$: the log-normal Gaussian with mean mass M .

Mass Func.	M (M_\odot)	$v_t = 190 \text{ km s}^{-1}$ $\langle t_E \rangle$	$v_t = 220 \text{ km s}^{-1}$ Γ_P/Γ_E	$\langle t_E \rangle$	Γ_P/Γ_E
HST					
$\delta(M)$	0.1	22.5	0.306	19.4	0.289
	0.5	50.3	0.201	43.4	0.191
$G(M)$	0.1	46.0	0.221	39.8	0.210
	0.5	57.1	0.194	49.3	0.184
$G(\log M)$	0.1	46.0	0.251	39.8	0.238
	0.5	51.2	0.200	44.2	0.190
VLT					
$\delta(M)$	0.1	22.5	0.122	19.4	0.104
	0.5	50.3	0.105	43.4	0.095
$G(M)$	0.1	46.0	0.108	39.8	0.096
	0.5	57.1	0.100	49.3	0.091
$G(\log M)$	0.1	46.0	0.108	39.8	0.095
	0.5	51.2	0.104	44.2	0.094

Note: The event time-scales $\langle t_E \rangle$ are given in day.

from comparing the event durations with the observed value $t_E \sim 40$ days. Then, the parallax effect can also be measured in $\sim 75\%$ (from the HST) and $\sim 60\%$ (from the VLT) of EAGLE events for the thin disc events. In Table 3, we also show that fractions in the case of $\delta = -367.5^\circ$ and $\Sigma_{\text{thick,thin}} = 50 M_\odot \text{ pc}^{-2}$ from the VLT. In this case the fractions are $\sim 30\%$ smaller than that in the case of $\delta = 45^\circ$.

For halo events, we adopt the mass function as a delta function $\delta(M)$, a Gaussian $G(M)$ and a log-normal Gaussian $G(\log M)$ distributions because the lens mass function is not well known. For $\delta(M)$ we adopt $M = 0.1$ and $0.5 M_\odot$. For $G(M)$ and $G(\log M)$ we take the mean of the mass $M = 0.1$ and $0.5 M_\odot$. The variance is $0.4 M_\odot$ for the $G(M)$ and $\log(0.4 M_\odot / M)$ for $G(\log M)$. Of course the mass function is zero for negative M in $G(M)$. The typical transverse velocity is $v_t = 190$ or 220 km s^{-1} . The estimated fractions in the case of $V < 25$ mag are shown in Table 4. The optical depth is 4.8×10^{-7} if $f = 1$. From Table 4, we can see that the fraction of parallax-measurable events out of all EAGLE events is $\sim 20\%$ (from the HST) and $\sim 10\%$ (from the VLT).

The fraction of parallax-measurable events depends on the lens location. Then we can also statistically discriminate whether the lenses are in the thick disc or halo, by using the parallax-measurable EAGLE event rate.

7 DISCUSSION AND CONCLUSION

We have seen that the EAGLE event rate is as high as that for normal events even for disc events towards the LMC. Since the period in which sources are visible ($V < 21$) is usually short (1 day ~ 40 days), the detection efficiency heavily depends on the observational frequency. The observational programs currently undertaken by most groups are

not adequate. Hourly monitoring with a 1-m class dedicated telescope and the real-time detection of EAGLE events by the DIA are required to issue alerts with a high detection efficiency. However, for the events in which the source star is $V > 25$ this period is less than 2 days, so it is difficult to detect. Thus we estimated Γ_E/Γ_N and Γ_P/Γ_E in the case that the source star is $V < 25$. These are decreased but still sufficiently high. Of course, the larger alert telescopes make it easier and faster to issue the alerts.

Estimating the parallax-measurable event rate, we advocate follow-up observations with a space telescope such as the HST and an 8-m class ground-based telescope such as the VLT. We have found that EAGLE events enlarge the opportunity of parallax measurements by $5 \sim 9$ (from the HST) and $6 \sim 10$ (from the VLT) times for disc events, and by ~ 8 (from the HST) and $4 \sim 6$ (from the VLT) times for halo events relative to that in normal microlensing events. We have also found we can measure the parallax effect in $\sim 75\%$ (from the HST) and $\sim 60\%$ (from the VLT) of EAGLE events if the lenses are in the thick or thin disc, and in $\sim 20\%$ (from the HST) and $\sim 10\%$ (from the VLT) if the lenses are in the halo. Since \tilde{v} for halo objects are $5 \sim 8$ times larger than that for disc stars, we can determine whether the lens objects are in the halo or discs for each event. We can also statistically constrain the lens locations by using the parallax-measurable EAGLE event rate.

In follow-up observations from the HST, in this paper we assumed that the observations start just after the peak as the most conservative case. Of course, an observation around the peak is better than that just after the peak. However predicting t_0 is not so easy for very faint source events. Extensive follow-up observations from small ground-based telescopes around the world are needed to predict t_0 and inform to the HST. Furthermore a flexible operating program of the HST for the alerts are required. If the alert telescope is at a latitude -30° , the alert can be issued for half of the year (Southern Summer), while at a latitude -44° (such as New Zealand) it can be done all year round. The total operation time of the HST would be several days per year.

From the VLT, we assumed $\delta = 45^\circ$. However for the events with faint source ($V > 24$) the time until t_0 is short, and the beginning of the follow-up would tend to be delayed. A delay of ~ 1 day reduces the possibility of measuring the parallax by $\sim 30\%$ as shown in §6.2. This observation can be done for only half of the year (Southern Summer).

The true source flux f_0 is needed to measure the precise value of \tilde{v} in the light curve fitting. Then follow-up observations by a high resolution telescope such as the HST are needed to get an accurate f_0 after the event.

In short, a practical observation strategy would be to observe hourly with a 1-m class telescope and perform real-time analysis with DIA to issue alerts to world observatories and the HST or the VLT for follow-up observations. Then after the events f_0 should be measured by the HST.

To demonstrate this specifically we estimate the number of expected parallax-measurable events for the two cases that these are mainly halo events or disc events. In both cases, the thin disc events are included. For the typical parameters $\alpha_d = 2.35$, $\Sigma_{\text{thin}} = \Sigma_{\text{thick}} = 50 M_\odot \text{ pc}^{-2}$, $V_{\text{th}} = 20$, a detection efficiency of 50% and source stars of $V < 25$, one can expect to find $\simeq 13$ EAGLE events from 3-year observations of 11 square degrees of the LMC central region (as the

Table 3. Fraction of parallax-measurable events in all EAGLE events and mean time-scales for disc events.

α_d	Σ_{thick} ($M_\odot \text{ pc}^{-2}$)	the thin disc				the thick disc			
		$M_1 = 0.1M_\odot$		$M_1 = 0.01M_\odot$		$M_1 = 0.1M_\odot$		$M_1 = 0.01M_\odot$	
		$\langle t_E \rangle$	Γ_P/Γ_E	$\langle t_E \rangle$	Γ_P/Γ_E	$\langle t_E \rangle$	Γ_P/Γ_E	$\langle t_E \rangle$	Γ_P/Γ_E
HST									
2.35	30	61.7	0.659	23.2	0.867	128.9	0.513	48.6	0.745
2.35	50	55.6	0.656	21.0	0.865	118.8	0.515	44.8	0.747
2.35	70	49.7	0.654	18.7	0.863	109.6	0.517	41.3	0.749
5.0	30	41.3	0.732	13.0	0.938	86.3	0.586	27.2	0.832
5.0	50	37.2	0.729	11.7	0.936	79.5	0.588	25.0	0.834
5.0	70	33.3	0.727	10.5	0.934	73.4	0.590	23.1	0.835
VLT ($\delta = 45^\circ$)									
2.35	30	61.7	0.486	23.2	0.704	128.9	0.355	48.6	0.580
2.35	50	55.6	0.479	21.0	0.687	118.8	0.356	44.8	0.575
2.35	70	49.7	0.469	18.7	0.664	109.6	0.355	41.3	0.566
5.0	30	41.3	0.555	13.0	0.785	86.3	0.421	27.2	0.668
5.0	50	37.2	0.546	11.7	0.765	79.5	0.420	25.0	0.660
5.0	70	33.3	0.532	10.5	0.736	73.4	0.418	23.1	0.648
VLT ($\delta = -367.5^\circ$)									
2.35	50	55.6	0.359	21.0	0.451	118.8	0.291	44.8	0.420
5.0	50	37.2	0.393	11.7	0.484	79.5	0.336	25.0	0.465

Note: The event time-scales $\langle t_E \rangle$ are given in day.

MACHO collaboration does). In the case of follow-up from the VLT, the expected number would be half. In these 13 EAGLE events, ~ 2 events (15%) are due to the stars in the thin disc and a further ~ 11 events are due to MACHOs or the dark stars in the thick disc. In considering these 11 events, reasonable parameters are $M = 0.1$ or $0.5M_\odot$ except $M = 0.1M_\odot$ in the case of the δ -function for halo events, and $M_1 = 0.01M_\odot$ for disc events, to be consistent with $\langle t_E \rangle \simeq 40$ days (Alcock et al. 2000b). In this case, we will be able to measure \tilde{v} in ~ 10 (from the HST) or ~ 4 (from the VLT) events for disc events, ~ 4 (from the HST) or ~ 1 (from the VLT) event for halo events, which include thin disc events. We can constrain lens locations strongly based on the 3-year statistics of these observations.

In conclusion, one could statistically discriminate whether the typical lens locations are in a thick disc or not, using parallax measurements even with $\sim R_\oplus$ scale baseline. One could also distinguish whether the lenses are MACHOs or stars in the LMC itself through finite source size effects measurements in EAGLE events (Sumi & Honma 2000). Therefore one could identify lens objects as halo MACHOs, dark stars in the Galactic thick disc, or stars in the LMC through these observations.

A real-time alert system with DIA, has been introduced by the MOA collaboration² from 2000 and by the OGLE collaboration³ from 2002.

ACKNOWLEDGMENTS

We are grateful to Y. Muraki for his supervision, and also to P. Yock and I. Bond for helpful comments. We would like to thank K. Sahu, B. Paczyński, L. Eyer and J. Tan for fruitful comments. We also acknowledge helpful discussions and continuous encouragement to Y. Sofue, S.M. Miyama, N. Sugiyama, and R. Nishi. T.S. acknowledge the financial support from the Nishina Memorial Foundation. We are also thankful to the referee for suggestive comments.

REFERENCES

- Afonso, C. et al. 2000, ApJ, 532, 340
- Alard, C. 2000, A&A, 144, 363
- Alard, C. & Lupton, R.H. 1998, ApJ, 503, 325
- Albrow, M.D. et al. 1999, ApJ, 512, 672
- Alcock, C. et al. 1995, ApJ, 454, 125
- Alcock, C. et al. 1997, ApJ, 486, 697
- Alcock, C. et al. 1999a, ApJ, 518, 44
- Alcock, C. et al. 1999b, ApJ, 521, 602
- Alcock, C. et al. 2000a, ApJ, 541, 734
- Alcock, C. et al. 2000b, ApJ, 542, 281
- Alcock, C. et al. 2001, ApJ, 552, 259
- An, J. H. et al. 2002, ApJ in press
- An, J. H., & Gould, A. 2001, ApJ, 563, L111
- Aubourg, É., Palanque-Delabrouille, N., Salati, P., Spiro, M., & Taillet, R. 1999, A&A, 347, 850
- Bahcall, J.N., Flynn, C., & Gould, A. 1992, ApJ, 389, 234
- Bennett, D.P. et al. 2001, preprint (astro-ph/0109467)
- Binney, J. & Tremaine, S. 1987, Galactic Dynamics (Princeton: NJ, Princeton University Press)

² see <http://www.phys.canterbury.ac.nz/~physib/alert/alert.html>

³ see <http://www.astrouw.edu.pl/~ogle/ogle3/ews/ews.html>

- Bond, I.A. et al. 2001, MNRAS, 327, 868
- Creze, M. 1998, A&A, 329, 920
- de Vaucouleurs, G. 1957, AJ, 62, 69
- Gates, E., Gyuk, G., Holder, G.P., & Turner, M.S. 1998, ApJ, 500, 145
- Gates, E., Gyuk, G. & Turner, M.S. 1995, Phys. Rev. D, 53, 4138
- Gilmore, G., & Reid, N. 1983, MNRAS, 202, 1025
- Gould, A. 1992, ApJ, 392, 442
- Gould, A. 1994a, ApJ, 421, 71
- Gould, A. 1994b, ApJ, 421, L75
- Gould, A. 1995a, ApJ, 440, 510
- Gould, A. 1995b, ApJ, 441, 21
- Gould, A. 1996, ApJ, 470, 201
- Gould, A. 1997, ApJ, 480, 188
- Gould, A. 1998, ApJ, 506, 253
- Gould, A., Miralda-Escude, J. & Bahcall, J.N. 1994, ApJ, 423, 105
- Gyuk, G., Dalal, N. & Griest, K. 2000, ApJ, 535, 90
- Han, C. 1997, ApJ, 490, 51
- Hansen, B.M.S. 1998, nature, 394, 860
- Hardy, S. J. & Walker, M. A. 1995, MNRAS, 276, L79
- Holmberg, J. & Flynn, C. 2000, MNRAS, 313, 209
- Holz, D.E. & Wald, R.M. 1996, ApJ, 471, 64
- Holtzman, J.A. 1997, AJ, 113, 656
- Honma, M. 1999, ApJ, 511, L29
- Honma, M. & Kan-ya, Y. 1998, ApJ, 503, L139
- Ioka, K., Tanaka, T. & Nakamura, T. 2000, ApJ, 528, 51
- Kuijken, K. & Gilmore, G. 1989, MNRAS 239, 605
- Mao, S. 1999, A&A, 350, L19
- Mao, S. et al. 2002, MNRAS, 329, 349
- Miyamoto, M., & Yoshii, Y. 1995, AJ, 110, 1427
- Miyamoto, M. & Zhu, Z. 1998, ApJ, 506, 253
- Nakamura, T. & Nishi, R. 1998, Progress of Theoretical Physics, vol.99, 963
- Nemiroff, R.J. & Wickramasinghe, W.A.D.T. 1994, ApJ, 424, 21
- Paczynski, B. 1986, ApJ, 304, 1
- Pavlovsky, C., et al. 2001, "ACS Instrument Handbook", Version 2.1, (Baltimore: STScI)
- Peng, E.W. 1997, ApJ, 475, 43
- Refsdal, S. 1966, MNRAS, 134, 315
- Sahu, K. 1994, PASP 106, 942
- Smith, M.C., Mao, S. & Woźniak, P.R. 2002, MNRAS, 332, 962
- Soszyński, I. et al. 2001, ApJ, 552, 731S
- Sumi, T. & Honma, M. 2000, ApJ, 538, 657
- Witt, H.J. & Mao, S. 1994, ApJ, 430, 505
- Woźniak, P.R. 2000, Acta Astronomica, 50, 421